Methods of stochastic geometry, and related statistical problems in Biology and Medicine

Vincenzo Capasso[1,2] and Alessandra Micheletti[1,2]

[1] Dipartimento di Matematica, Università degli Studi di Milano,
Via C. Saldini, 50, 20133 Milano, Italy,
[2] ADAMSS (Advanced Applied Mathematical and Statistical Sciences)
Vincenzo.Capasso@unimi.it, Alessandra.Micheletti@unimi.it

1 Introduction

In his pioneering book entitled "On Growth and Form", [DT17], D'Arcy Thompson claimed that "THERE IS AN IMPORTANT RELATIONSHIP BETWEEN THE FORM OR SHAPE OF A BIOLOGICAL STRUCTURE AND HIS FUNCTION". This leads to the important idea that in Biomedicine the analysis of the morphology of patterns may lead to the diagnosis of malfunctioning of an organ or organism. Actually many processes of interest are, in general, stochastic both in time and space, so that a statistical analysis of stochastic geometries is required.

The scope of this presentation is then to introduce relevant nomenclature and mathematical methods for the analysis of geometries related to patterns of biomedical interest, thus providing a guided tour in a selected bibliography.

First of all let us introduce the current terminology in this framework.

As a working example let us consider the analysis of the random network associated with vasculogenesis and tumor-driven angiogenesis (see Figures 1,2, 3, 4). The study of angiogenesis has such potential for providing new therapies that it has received enthusiastic interest from the pharmaceutical and biotechnology industries. Many of the compounds now under investigation inhibit angiogenesis and thus the growth of the cancer.

These structures induce a random division of the relevant spatial region, known as random tessellation (see Figures 4,5). A quantitative description of the spatial structure of a tessellation can be given, in terms of the mean densities of interfaces (n-facets; $n = 0$ for vertices, $n = 1$ for lines – edges, fibers, etc. – $n = 2$ for faces, and so on, up to the full dimension d of the relevant space).

Statistical methods for the estimation of vessel densities may offer significant tools for diagnosis, and dose/response analysis in medical treatments.

We will present a mathematical framework for modelling random geometric structures, so to define in a rigorous way geometric densities of such

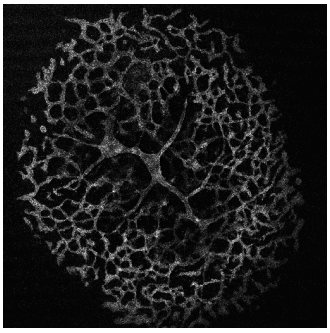

Fig. 1. Vascularization of an allantoid (from [CFD99]).

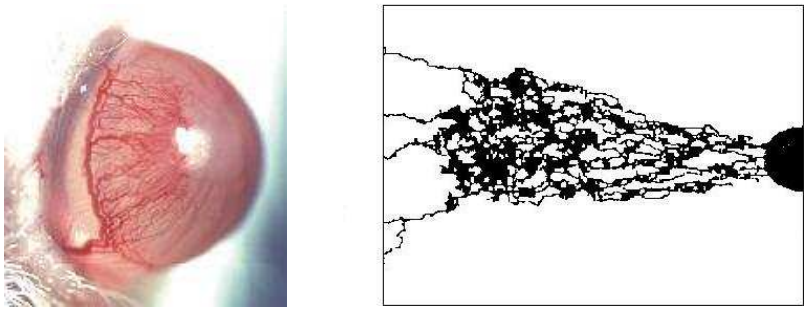

Fig. 2. Angiogenesis on a mouse cornea [Credit: Dejana et al [CZD02]] (left). A simulation of an angiogenesis due to a localized tumor mass (black region on the right) (from [CA99])(right).

structures. Correspondingly we propose statistical estimators of such densities which, in general, are not spatially homogeneous(see e.g. [BR04]).

In the modelling and statistical analysis of the above mentioned systems it is of great importance to handle random closed sets of different (even though integer) Hausdorff dimensions, usually smaller than the dimension $d \in \mathbb{N}$ of the relevant space.

Here an original approach is reported, recently proposed by the authors, who have suggested to cope with these problems by introducing generalized densities (distributions) *á la Dirac-Schwartz*, for both the deterministic case and the stochastic case. In this last one, mean generalized densities are meaningful [CV07, ACV06].

The above approach also suggests methods for the statistical estimation of geometric densities of the stochastic fibre system that characterize the morphology of a real vascular system. Here we apply such methods to real data,

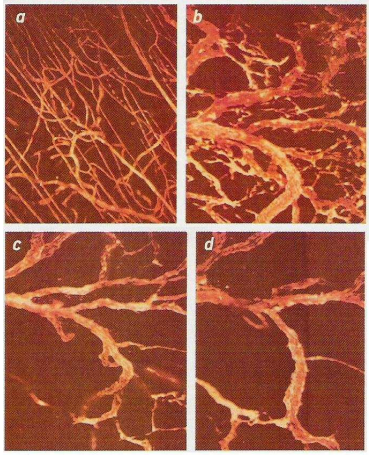

Fig. 3. Response of a vascular network to an antiangiogenic treatment (from [JC01]).

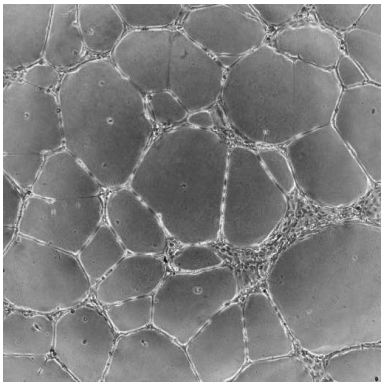

Fig. 4. A real picture showing a spatial tessellation due to vascularization of a biological tissue: endothelial cells form a vessel network (from [Ser03]). See also Fig. 5 for a simulation of a stochastic tessellation generated by a birth-and-growth process.

taken from the literature, and to simulated data, obtained by existing computational models of tumor-induced angiogenesis; indeed these methods can be used for validating computational models, and for monitoring the efficacy of possible medical treatment [CM08].

In Section 2 basic concepts of stochastic geometry have been introduced. In Sections 3, 4, based on a theory of random distributions *á la Dirac-Schwartz*, mean geometric densities are defined for absolutely continuous random sets. In Section 5 applications to the study of random tessellations are presented.

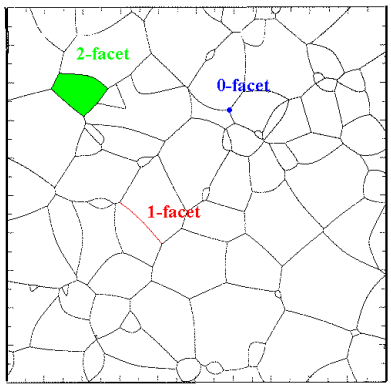

Fig. 5. $n-$facets for a tessellation in $\mathbb{R}^2$

Section 6 is devoted to the presentation of an original statistical approach for estimating geometric densities of stochastic fibre systems, that characterize the morphology of a real vascular system. In Section 7 a series of experimental results are reported, which show the power of this approach for the estimation of such densities for vascular systems, either real or simulated.

2 Stochastic Geometry

A relevant aspect of stochastic geometry is the analysis of the spatial structure of objects which are random in location and shape. Given a random object $\Sigma \in \mathbb{R}^d$, a first quantity of interest is for example the probability that a point x belongs to Σ, or more in general the probability that a compact set K intersects Σ.

The theory of Choquet-Matheron [Mat75, SKM95], shows that it is possible to assign a unique probability law P_Σ associated with a *RACS* (*random closed set*) $\Sigma \in \mathbb{R}^d$ on the measurable space $(\mathcal{F}, \sigma_\mathcal{F})$ of the family of closed sets in $\mathbb{R}^d$ endowed with the σ-algebra generated by a suitable topology, by assigning its *hitting functional* T_Σ. Given a probability space $(\Omega, \mathcal{A}, P)$, a RACS Σ is a measurable function

$$\Sigma : (\Omega, \mathcal{A}) \longrightarrow (\mathcal{F}, \sigma_\mathcal{F}).$$

The hitting functional of Σ is defined as

$$T_\Sigma : K \in \mathcal{K} \longmapsto P(\Sigma \cap K \neq \emptyset),$$

where $\mathcal{K}$ is the family of compact sets in $\mathbb{R}^d$.

We shall denote by $\mathbb{E}_\Sigma$, or simply by $\mathbb{E}$, the expected value with respect to the probability law P_Σ.

We may estimate directly the hitting functional $T_{\Theta^t}(K)$, for a sufficiently large family of compact sets K and for different time instants t, as follows. In Figure 6 the hitting functional has been estimated for a naive simulated example of tumor driven angiogenesis; vessels are growing from left to right driven by a tumor located along the left side of the shown window. Due to the vertical homogeneity we have divided the window of observation into (locally) homogeneous subwindows, and overlapped to any of them a lattice of points $x_1, \ldots, x_n$ such that $(K \oplus x_i) \cap (K \oplus x_j) = \emptyset$, for any $i \neq j$. For each subwindow we have computed the following estimator

$$\hat{T}_{\Theta^t}(K) = \frac{1}{n} \sum_{i=1}^{n} \mathbf{1}_{[(K \oplus x_i) \cap \Theta^t \neq \emptyset]}.$$

This is a generalization of a classical estimator of $\hat{T}_{\Theta^t}(\{x\})$ proposed in the relevant literature (see e.g. [SKM95]).

In several real applications it is of interest to study random closed sets of different Hausdorff dimensions. For definitions and basic properties of Hausdorff measure and Hausdorff dimension see, e.g., [AFP00, Fal85, Fed96]. Denoting by $\mathcal{H}^n$ the n-dimensional Hausdorff measure, we recall that $\mathcal{H}^0$ is the usual counting measure; for any Borel set $B \subset \mathbb{R}$, $\mathcal{H}^d(B)$ coincides with the usual d-dimensional Lebesgue measure of B; for $1 \leq n < d$ integer, $\mathcal{H}^n(B)$ coincides with the classical n-dimensional measure of B if $B \in \mathcal{B}_{\mathbb{R}^d}$ (the Borel σ-algebra of $\mathbb{R}^d$) is contained in a C^1 n-dimensional manifold embedded in $\mathbb{R}^d$. Further, we recall that the Hausdorff dimension of a set $A \subset \mathbb{R}^d$ is defined as

$$\dim_{\mathcal{H}}(A) := \inf\{0 \leq s < \infty \,|\, \mathcal{H}^s(A) = 0\},$$

so that, in particular, a point has Hausdorff dimension 0, a curve (or a fibre) has Hausdorff dimension 1, a hypersurface in $\mathbb{R}^d$ has Hausdorff dimension $d-1$. Note that the Hausdorff dimension of a set A need not to be an integer (e.g., consider the Cantor set), and $\dim_{\mathcal{H}}(A) = s$ does not imply that $\mathcal{H}^s(A)$ is positive and finite (we may have $\dim_{\mathcal{H}}(A) = s$ and $\mathcal{H}^s(A) = 0$, or $\mathcal{H}^s(A) = \infty$).

We say that a random closed set Θ has Hausdorff dimension n if $\dim_{\mathcal{H}}\Theta(\omega) = n$ for a.e. $\omega \in \Omega$; in such case, in the following we also write Θ_n to remind its Hausdorff dimension.

3 Generalized densities

In the sequel we will refer to a class of sufficiently regular random closed sets in the Euclidean space $\mathbb{R}^d$, of integer dimension n. We denote by $B_r(x)$ the ball with center x and radius r; b_n denotes the volume of the unit ball in $\mathbb{R}^n$. If A_n is a sufficiently regular (deterministic) closed set in $\mathbb{R}^d$, having Hausdorff dimension $n < d$, we have

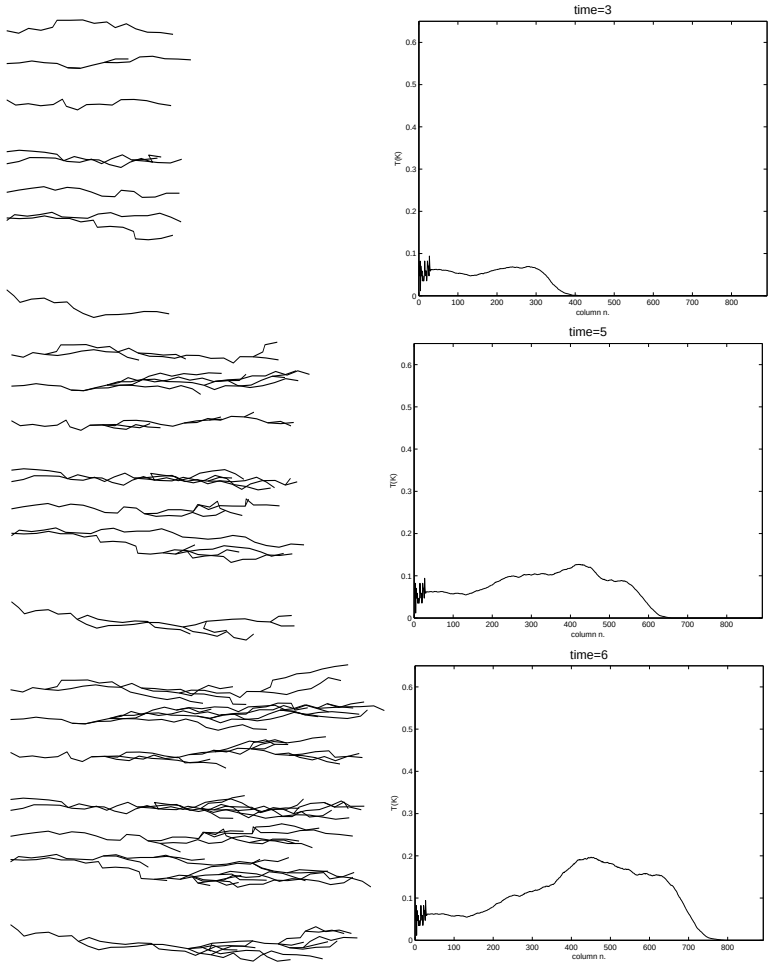

Fig. 6. Estimate of the hitting functional $\hat{T}_{\Theta^t}(K)$, for different instants t of a (naive) simulation of an angiogenesis, whose vessels develop from the left to the right. The chosen compact set K is a vertical segment of length 6 pixels, which has been moved into vertical stripes in the pictures, which show a vertical spatial homogeneity.

$$\lim_{r\to 0}\frac{\mathcal{H}^n(A_n\cap B_r(x))}{b_d r^d}=\lim_{r\to 0}\frac{\mathcal{H}^n(A_n\cap B_r(x))}{b_n r^n}\frac{b_n r^n}{b_d r^d}$$
$$=\begin{cases}\infty & \mathcal{H}^n\text{-a.e. } x\in A_n,\\ 0 & \forall x\notin A_n.\end{cases}$$

so that, in analogy with the usual Dirac delta function $\delta_{x_0}(x)$ associated with a point $x_0\in\mathbb{R}^d$ (a 0-regular closed set), we may introduce the following definition [KF70].

Definition 1 (Generalized density). *We call* generalized density *(or, briefly,* density*) associated with A_n, the quantity δ_{A_n}, defined by*

$$\delta_{A_n}(x) := \lim_{r\to 0} \frac{\mathcal{H}^n(A_n \cap B_r(x))}{b_d r^d},$$

finite or not.

If Θ_n is a random closed set in $\mathbb{R}^d$, the measure

$$\mu_{\Theta_n}(\cdot) := \mathcal{H}^n(\Theta_n \cap \cdot)$$

is a random measure, and consequently $(\delta_{\Theta_n}, f) = \int_{\mathbb{R}^d} f(x)\delta_{\Theta_n}(x)\,\mathrm{d}x$, is a real random variable for any test function f.

A formal definition of *mean generalized density* can be given by considering the expected value of the random measure $\mathcal{H}^n(\Theta_n \cap \cdot)$

$$\mathbb{E}[\delta_{\Theta_n}](x) := \lim_{r\to 0} \frac{\mathbb{E}[\mathcal{H}^n(\Theta_n \cap B_r(x))]}{b_d r^d}.$$

It can be shown [CV08] that for any test function f, we have

$$\int_{\mathbb{R}^d} f(x)\mathbb{E}[\delta_{\Theta_n}](x)\,\mathrm{d}x = \mathbb{E}\left[\int_{\mathbb{R}^d} f(x)\delta_{\Theta_n}(x)\,\mathrm{d}x\right];$$

so that, formally, we may exchange integral and expectation.

The case of interest in applications [BR04, Mol92, Hahn99] is the one in which the mean generalized density is a classical function.

When $n = d$, a classical mean density always exists, and it is known as volume density $V_V(x) := \mathbb{P}(x \in \Theta_d)$; in material science it is known as the *(degree of) crystallinity* [Avr39, K37].

In a tessellation (see Section 5), $\mathbb{E}[\delta_{\Theta_n}(x)]$ is known as *n-facet density*, for any other integer $0 \le n \le d-1$; for fibre processes ($n = 1$) we speak of fibre density, etc. Figure 7 shows the estimation of the evolution of the vessel density for the simulation in Figure 2, by means of the estimators proposed in Section 6.

4 Approximation of mean densities

In many real applications (see e.g. [BR04] and [SKM95]), it is of interest the estimation of the local mean density $\mathbb{E}[\delta_{\Theta_n}]$ of a lower dimensional random closed set such as a fibre process of dimension $n = 1$ in a space of dimension $d > 1$.

For facing the problem of the zero ν^2-measure for points or lines in $\mathbb{R}^2$ it is natural to make use of their 2-D box approximations. As a matter of fact, a computer graphic representation is usually provided in terms of pixels, which can only offer a 2-D box approximation of points or lines in $\mathbb{R}^2$.

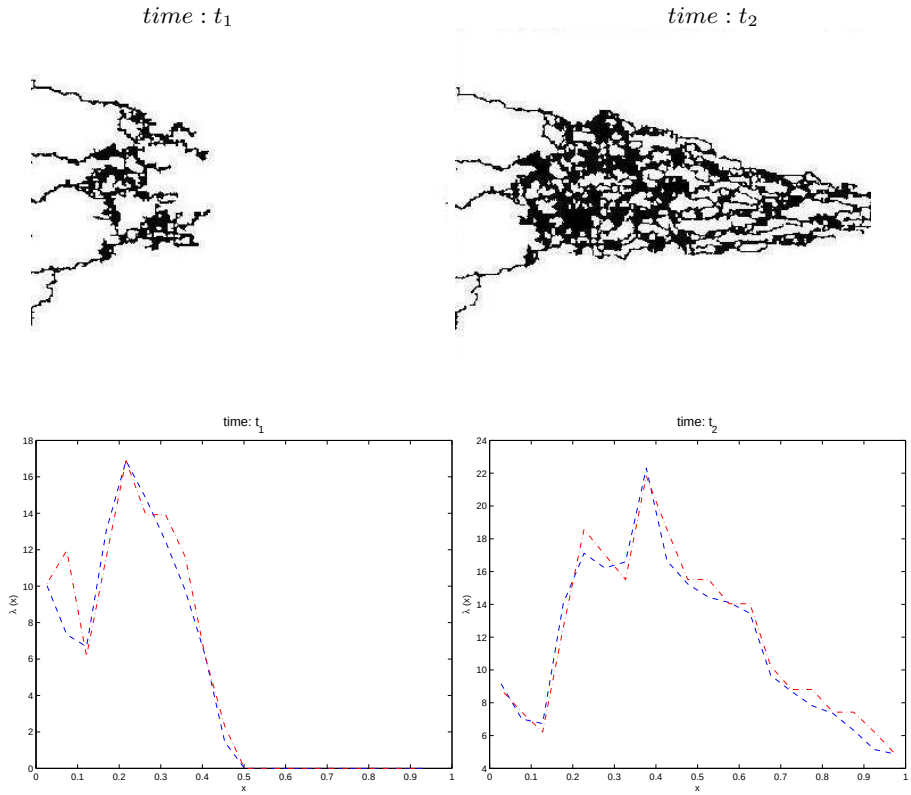

Fig. 7. Estimate of the density(mean length per unit area) of fibres, at two different instants of a simulation of a tumor-driven angiogenesis, taken from [CA99]. The estimators are described in Section 6. Dashed line= $\hat{\lambda}^1_{k,r,p}$, dotted-dashed line= $\hat{\lambda}^2_{k,r,p}$

Thus, given a random closed set Θ_n with Hausdorff dimension $n < d$, we will consider the enlarged set $\Theta_{n_{\oplus r}}$, which is now of dimension d, and hence of nontrivial measure ν^d.
On the other hand, we may observe that $\mathbb{P}(x \in \Theta_{n_{\oplus r}}) = T_{\Theta_n}(B_r(x))$, where T_{Θ_n} is the hitting functional associated to Θ_n, which characterizes the probability structure of the random set Θ_n.

According to [CV06a], if Θ_n admits a classical mean density λ_{Θ_n}, for all $A \in \mathcal{B}_{\mathbb{R}^d}$,

$$\mathbb{E}[\mathcal{H}^n(\Theta_n \cap A)] = \int_A \lambda_{\Theta_n}(x)\,\mathrm{d}x.$$

In this case, we have that

$$\lim_{r\to 0} \int_A \frac{T_{\Theta_n}(B_r(x))}{b_{d-n} r^{d-n}} \mathrm{d}x = \int_A \lambda_{\Theta_n}(x)\,\mathrm{d}x. \tag{1}$$

If Θ_n is a stationary random closed set, then $T_{\Theta_n}(B_r(x))$ is independent of x and the expected measure $\mathbb{E}[\mu_{\Theta_n}]$ is motion invariant, hence it admits density $\lambda_{\Theta_n}(x) = L \in \mathbb{R}_+$ for ν^d-a.e. $x \in \mathbb{R}^d$. It follows that

$$\lim_{r \to 0} \frac{T_{\Theta_n}(B_r(0))}{b_{d-n} r^{d-n}} = L.$$

5 Mean densities of stochastic tessellations

Stochastic tessellations are a natural consequence of the random division of space due to the establishment of a vessel network in vasculogenesis (see Figure 4). A random subdivision of space needs further information to be characterized. In this case the spatial region in $\mathbb{R}^d$ where the relevant process occurs is randomly divided into cells (e.g. in a random Johnson-Mehl tessellation [JM39, Mol92]; see also [Mol94]), and interfaces (n-facets, $n = 0, 1, \cdots, d$) at different Hausdorff dimensions (cells, faces, edges, vertices) appear (for a planar process, see Figure 5).

As above, we may describe quantitatively the tessellation by means of mean densities of the n-facets [Mol92].

We may call **cell** of a random tessellation any element of a family of RACS's partitioning the region E in such a way that any two distinct elements of the family have empty intersection of their interiors.

Let us now introduce a rigorous concept of "interface" at different Hausdorff dimensions.

Definition 2. *An* **n-facet** *at time t* $(0 \leq n \leq d)$ *is the non-empty intersection between* $m+1$ *cells, with* $m = d - n$.

Note that in the previous definition

- $d =$ dimension of the space in which the tessellation takes place
- $n =$ Hausdorff dimension of the interface under consideration
- $m + 1 =$ number of cells that form such an interface
- for $n = d$ a d-facet is simply a cell

(see also Figure 5).

For a system which evolves in time, we may consider the union of all n-facets at time t, $\Xi_n(t)$. For any Borel set B in $\mathbb{R}^d$ one can define the *mean n-facet content* of B at time t as the measure

$$\mathcal{M}_{d,n}(t, B) = \mathbb{E}\left[\mathcal{H}^n(B \cap \Xi_n(t))\right] \tag{2}$$

where $\mathcal{H}^n$ is the n-dimensional Hausdorff measure.

Suppose that the process is such that $\mathcal{M}_{d,n}$ admits a density $\mu_{d,n}(t, x)$ with respect to ν^d, the standard d-dimensional Lebesgue measure on $\mathbb{R}^d$, i. e. for any Borel set B

$$\mathcal{M}_{d,n}(t,B) = \int_B \mu_{d,n}(t,x)dx, \tag{3}$$

then the following definition is meaningful.

Definition 3. *The function $\mu_{d,n}(t,x)$ defined by (3) is called local mean n-facet density of the tessellation at time t.*

In particular $\mu_{d,d-1}(t,x)$ is the surface density of the cells.

6 Statistical methods for fibre systems

We now describe some statistical methods which furnish a quantitative description of the mean geometric characteristics of random fibre systems, which, at a suitable scale where the width of the fibres can be neglected (i.e. fibres have Hausdorff dimension 1), may represent networks of vessels generated by angiogenesis or vasculogenesis, or also other networks, for example of neurons, lymph vessels, etc. Since in most cases such networks have a spatially non homogeneous structure, statistical methods which may put into evidence and compare quantitatively spatial inhomogeneities are a valid tool both for medical doctors, for diagnosis and dose/response analysis and thus therapy, and for mathematicians, to validate mathematical models by comparison of simulated and real data. One of the first descriptors of the mean geometry of a random fibre system is its mean length density, also called *intensity*, of which here we will describe some estimators.

Let Γ be a *random fibre system* in $\mathbb{R}^d$ (see [BR04] or [CM08] for the definition).

Note that

$$T_\Gamma(B_r(x)) = \mathbb{P}(x \in \Gamma_{\oplus r}) = \mathbb{P}(\Gamma \cap B_r(x) \neq \emptyset)$$

where $\Gamma_{\oplus r}$ is the parallel set of Γ having width r. We may rewrite Equality (1), for $\Theta_n = \Gamma$ and $n = 1$, in the following ways

$$\int_A \lambda_\Gamma(x)dx = \lim_{r\to 0} \int_A \frac{T_\Gamma(B_r(x))}{b_{d-1}r^{d-1}}dx \tag{4}$$

$$= \lim_{r\to 0} \int_A \frac{\mathbb{P}(x \in \Gamma_{\oplus r})}{b_{d-1}r^{d-1}}dx \tag{5}$$

$$= \lim_{r\to 0} \int_A \frac{\mathbb{P}(\Gamma \cap B_r(x) \neq \emptyset)}{b_{d-1}r^{d-1}}dx \tag{6}$$

Equalities (4)-(6) provide a way to introduce estimators of $\lambda_\Gamma(x)$ for a random fibre, or fibre system Γ, provided that the limit and the integrals in the right-hand terms of (4)-(6) can be exchanged, by estimating the quantities

$$\frac{T_\Gamma(B_r(x))}{b_{d-1}r^{d-1}} = \frac{\mathbb{P}(x \in \Gamma_{\oplus r})}{b_{d-1}r^{d-1}} = \frac{\mathbb{P}(\Gamma \cap B_r(x) \neq \emptyset)}{b_{d-1}r^{d-1}}.$$

We will call them *histogram-like* estimators, since the "enlargement" $\Gamma_{\oplus r}$ of the set Γ via the Minkowski addition of a d-dimensional ball, which approximates the fibre with a d-dimensional set, imitates the procedure used when we estimate the p.d.f. of a real random variable from an i.i.d. sample using moving histograms or kernels (see [Hard91, Pest98, Silv86] for details), where we "enlarge" the Dirac-delta's measures concentrated on the sample points, approximating them with classical and sufficiently regular functions.

According to the definitions introduced in the previous sections, the density of Γ is defined by

$$\lambda_\Gamma(x) = \mathbb{E}[\delta_\Gamma](x) = \lim_{r\to 0} \frac{\mathbb{E}(\mathcal{H}^1(\Gamma \cap B_r(x)))}{r^d b_d}.$$

In the following we will provide two estimators for the density of a random fibre system Γ, based on the estimate of $T_\Gamma(B_r(x))$ or of $\mathbb{P}(\Gamma \cap B_r(x) \neq \emptyset)$.

Basic assumptions for the estimation procedure

Suppose to have one or more images of the random fibre system Γ under study and that the window $W \subseteq \mathbb{R}^d$ where Γ is observed can be divided in a partition of subwindows $\{A_k\}_{k=1,\dots,K}$ such that

A1 $A_j \cap A_k = \emptyset, \quad \forall j \neq k$
A2 $\bigcup_{k=1}^K A_k = W$
A3 in each window A_k limit and integral in (1) can be exchanged when $\Theta_n = \Gamma$
A4 the density $\lambda_\Gamma(x)$ can be locally well approximated by piecewise constant functions, assuming different constant values in each window A_k.

Note that Assumption A3 is satisfied if in A_k the fibre system is (*locally*) stationary at a suitable mesoscale (see [ACV06] for a discussion of this problem).

6.1 Estimators of the density

Let us assume A1-A4; then for all $x \in A_k$, let us denote by λ_k the (constant) density of the random fibre system in the subwindow A_k. We will obtain two different estimators, based on the estimate of the quantities

1. $\mathbb{P}(x \in \Gamma_{\oplus r} \cap A_k)$
2. $T_\Gamma(B_r(x))$,

respectively.

Fattening fibres

Let us build first an estimator based on the estimate of $\mathbb{P}(x \in \Gamma_{\oplus r} \cap A_k)$. Let us overlap to A_k a grid of points $z_1, \ldots, z_p \in A_k$ and build the set $\Gamma_{\oplus r} \cap A_k$. Then a first estimator of λ_k is

$$\hat{\lambda}^1_{k,r,p} := \frac{1}{2rp} \sum_{i=1}^{p} \mathbf{1}_{z_i \in \Gamma_{\oplus r} \cap A_k} \tag{7}$$

where $\mathbf{1}_{z_i \in \Gamma_{\oplus r} \cap A_k}$ are Bernoulli random variables assuming value one with probability $\mathbb{P}(x \in \Gamma_{\oplus r} \cap A_k)$ which is independent of $x \in A_k$ in our assumptions.

The asymptotic unbiasedness and other relevant statistical properties of this estimator can be easily proven (see [CM09] for the proofs, and a discussion on edge effects).

Fattening points

Let us now introduce an estimator based on the estimate of $T_\Gamma(B_r(x)), x \in A_k$.

Let us again consider a grid of points $z_1, \ldots, z_p$ overlapped on the window A_k, such that $B_r(z_i) \subseteq A_k$ for all $i = 1, \ldots, p$ (this assumption has the aim of reducing the edge effects). We then define

$$\hat{\lambda}^2_{k,r,p} := \frac{1}{2rp} \sum_{i=1}^{p} \mathbf{1}_{\Gamma \cap B_r(z_i) \neq \emptyset} \tag{8}$$

where again $\mathbf{1}_{\Gamma \cap B_r(z_i) \neq \emptyset}$ is a Bernoulli random variable assuming value 1 with probability $\mathbb{P}(\Gamma \cap B_r(z_i) \neq \emptyset) = T_\Gamma(B_r(z_i)) = T_\Gamma(B_r(x))$, $\forall x \in A_k$.

Again this is an asymptotically unbiased estimator (see [CM09]).

Both estimators can be computed by overlapping either a grid of deterministic and equally spaced points $z_1, \ldots, z_p$, or a random grid of points uniformly distributed on a window of observation. For a discussion of the advantages of either methods see [CM09].

7 Application of the estimators to simulated angiogenic processes

The estimators have then been applied to some (naive) simulations of real fibre processes , where the simulation of the generation and branching of vessels driven by a chemotactic field generated by a tumor is reported [CM08]. The tumor is located on the right hand side of the window and the vessels start growing and branching from the left hand side of the window in the right direction. The chemotactic field has a gradient in the x direction and

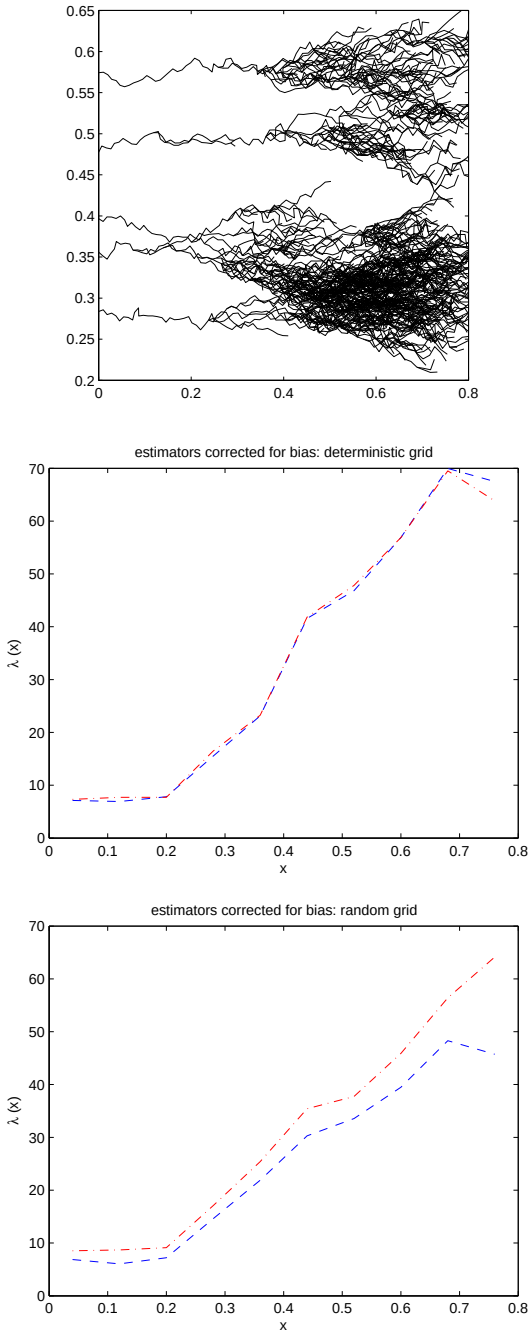

Fig. 8. Estimate of the fibre density of an angiogenic process with a chemotactic field having a gradient in the x direction. Middle figure: estimate with a deterministic grid; bottom figure:estimate with a random grid of 2000 points. The estimators have been corrected for bias. Dashed line= $\hat{\lambda}^1_{k,r,p}$, dotted-dashed line= $\hat{\lambda}^2_{k,r,p}$

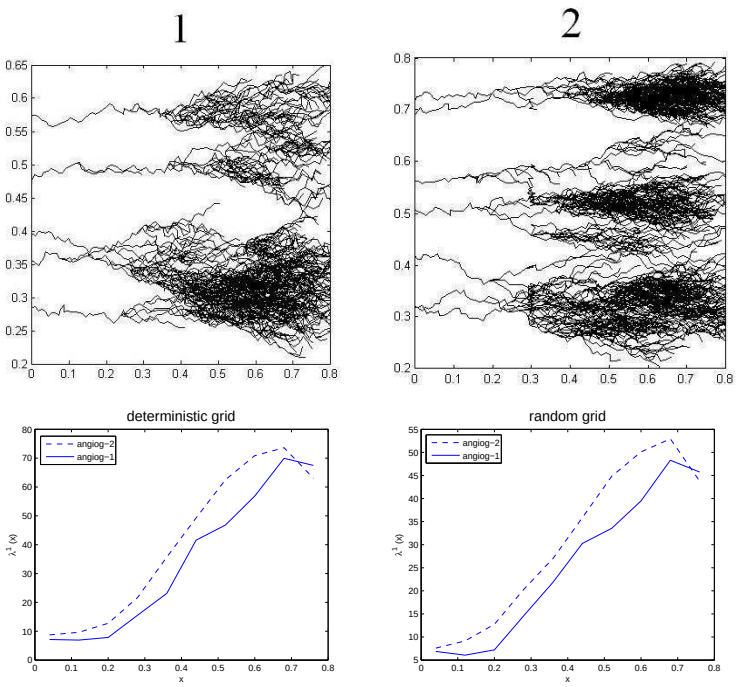

Fig. 9. Comparison between the two simulated angiogenic processes depicted in the top line. Bottom left: comparisons of $\hat{\lambda}^1_{k,r,p}$ for the two processes estimated with a deterministic grid; bottom right: comparisons of $\hat{\lambda}^1_{k,r,p}$ for the two processes estimated with a random grid. In both cases the first process reveals a density lower than the second, and this was really the case in the performed simulation.

influences both the speed of growth and the branching of the vessels. The density has been estimated both with a deterministic and a random grid, by dividing the observation window into 10 vertical stripes of the same width. The estimators have been corrected for bias. The results are reported in Figure 8. In Figure 9 two simulations are reported where the intensities of branching where different. The difference is not much evident by simply looking at the patterns, but the estimate of the density reveals that the pattern on the left has a lower density than the pattern on the right for any value of x, and this was really the case, since the frequency of branching and speed of growth was settled higher in the right hand pattern. This is thus an example where quantitative analysis is essential for the characterization and differentiation of the geometry.

In Figure 10 an analogous process but driven by a chemotactic field with a spherical symmetry around a point-shaped tumor is reported. Because of the observed symmetry, in this case the window of observation has been divided

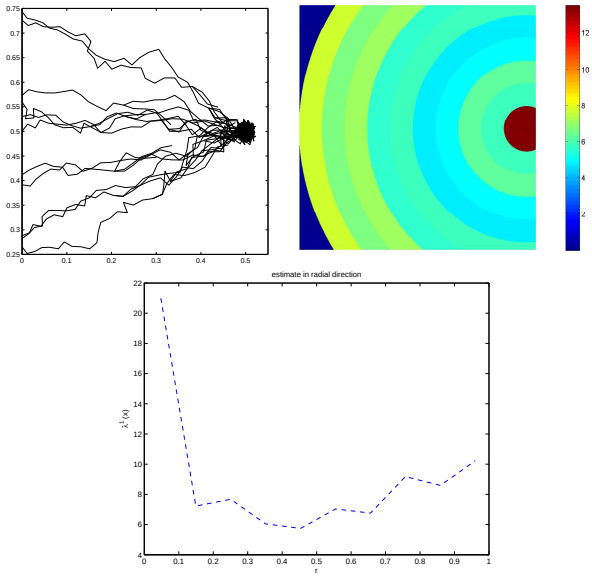

Fig. 10. Estimate of the fibre density of an angiogenic process driven by a chemotactic field with a spherical symmetry. Top line: the fibre process and an estimate of $\hat{\lambda}^1_{k,r,p}$ using a random grid and dividing the window into 10 spherical shells centered at the tumor; bottom: plot of $\hat{\lambda}^1_{k,r,p}$ with respect to the radial coordinate, centered at the tumor

into 10 spherical shells centered at the tumor location. Both the estimated values in each subregion in a 2D visualization and the plot of the estimated density with respect to the radial coordinate are reported. In this case, since the subwindows are spherical shells, only estimator $\hat{\lambda}^1_{k,r,p}$ has been computed, since it is more easily computable for non-rectangular regions (see [CM09]).

In Figures 11, 12,13 a simulated angiogenic fibre system is shown and the set of branching points (for simplicity only branching is simulated and not anastomosis).

In Figure 14 estimator $\hat{\lambda}^1_{k,r,p}$ has been computed on three images of a vascular networks generated in allantoids (see [CM06] for a discussion of the relevance of these studies in tumor treatment). Two of the three allantoids have been treated with two different doses of an antiangiogenic substance, which should inhibit the formation of vessels. The figure on the left refers to an untreated control allantoid. Because of the spherical symmetry of the images, also in this case the observation window has been divided into spherical shells centered at the centroid of the allantoid. The results of the estimate reveal, in a quantitative way, that the increase of the dose of the substance results in a less widespread network and in a lower density of length of the vessels.

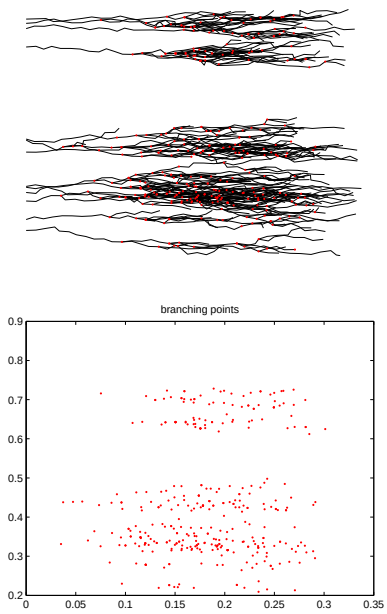

Fig. 11. A simulated angiogenic process (left). Branching points related to the simulated process(right).

Acknowledgements

It is a pleasure to acknowledge useful discussions with many Colleagues, at different Universities and Research Centres. Particular thanks are due to Professor Luigi Ambrosio (SNS, Pisa), and Dr. Elena Villa (Milan).

References

[ACV06] Ambrosio, L., Capasso, V., Villa, E.: On the approximation of geometric densities of random closed sets. RICAM Report N. 2006-14,Linz,Austria (2006). Bernoulli (2009).In press.

[AFP00] Ambrosio, L., Fusco, N., Pallara, D.: Functions of Bounded Variation and Free Discontinuity Problems. Clarendon Press, Oxford (2000).

[Avr39] Avrami, M.: Kinetics of phase change. Part I, J. Chem. Phys. **7**, 1103–112 (1939).

[BR04] Beneš, V., Rataj, J.: Stochastic Geometry. Kluwer, Dordrecht (2004).

[CM08] Capasso, V., Dejana, E., Micheletti, A. (2008). Methods of stochastic geometry, and related statistical problems in the analysis and therapy of tumour

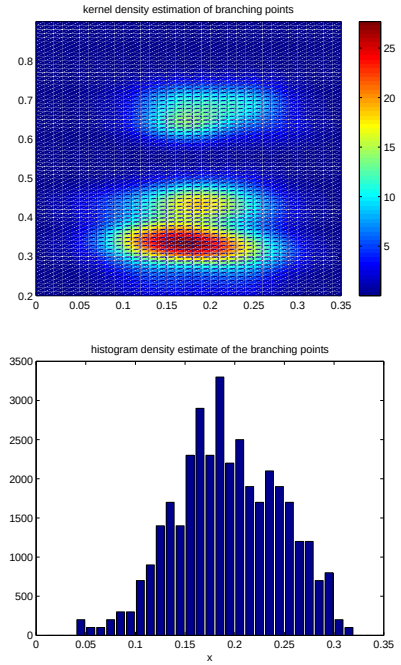

Fig. 12. The kernel estimate of the local spatial density of vertices of the simulation above (left). Histogram of the number of vertices along vertical bands (right).

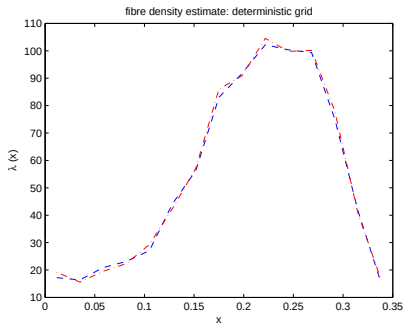

Fig. 13. Estimate of the local spatial density of vessels of the simulation above, by means of the two proposed estimators.

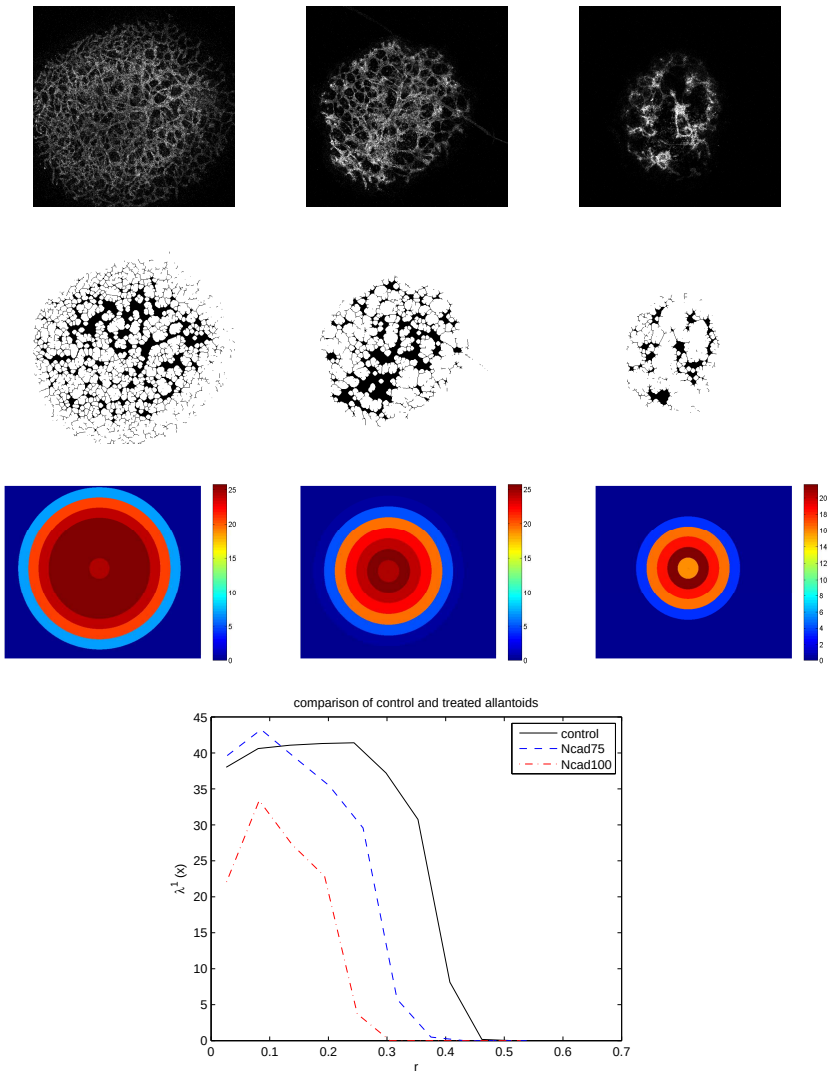

Fig. 14. Vascularization in allantoids. First line, from left to right: control experiment (untreated), treated with 0.75 mg of antiangiogenic substance, treated with 1 mg of antiangiogenic substance [Credit: [CFD99]]. Second line: scheletonization of the upper images. Third line: 2D representation of the density estimate of the fibres in the skeletons; the space has been divided into 10 spherical concentric shells. Bottom line: comparison of the radial estimates of the intensities of the 3 allantoids

growth and tumour-driven angiogenesis, in *Selected Topics on Cancer Modelling. Genesis-Evolution-Immune Competition-Therapy* (eds. N. Bellomo, M. Chaplain, E. De Angelis),Birkhauser, Boston, pp. 299-335.

[Cap03] Capasso, V. (ed): Mathematical Modelling for Polymer Processing. Polymerization, Crystallization, Manufacturing. Mathematics in Industry, Vol.2, Springer-Verlag, Heidelberg (2003).

[CM06] Capasso, V., Micheletti, A.: Stochastic geometry and related statistical problems in Biomedicine. In: A. Quarteroni et al(eds) Complex Systems in Biomedicine. Springer, Milano, 36–69 (2006).

[CM09] Capasso, V., Micheletti, A.: Kernel-like estimators of the mean density of inhomogeneous fibre processes. In preparation(2009).

[CV06a] Capasso, V., Villa, E.: On the continuity and absolute continuity of random closed sets. Stoch. Anal. Appl.,**24**, 381–397 (2006a).

[CV07] Capasso, V., Villa, E.: On mean densities of inhomogeneous geometric processes arising in material science and medicine - Image Analysis And Stereology, **26**, 23–36 (2007).

[CV08] Capasso, V., Villa, E.: On the geometric densities of random closed sets. Stoch. Anal. Appl., **27**, 784–808 (2008).

[CA99] Chaplain, M.A.J., Anderson, A.R.A.: Modelling the growth and form of capillary networks. In: Chaplain, M.A.J. et al (eds) On Growth and Form. Spatio-temporal Pattern Formation in Biology. John Wiley & Sons, Chichester (1999).

[CZD02] Corada, M., Zanetta,L., Orsenigo, F., Breviario,F., Lampugnani,M.G., Bernasconi,S., Liao,F., Hicklin,D.J., Bohlen,P., and Dejana,E.: A monoclonal antibody to vascular endothelial-cadherin inhibits tumor angiogenesis without side effects on endothelial permeability. Blood. **100**,905–911 (2002)

[CFD99] Crosby, C.V., Fleming, P., Zanetta,L., Corada, M., Giles, B., Dejana, E., Drake, C.: VE-cadherin is essential in the de novo genesis of blood vessels (vasculogenesis) in the allantoids. Blood **105**, 2771–2776 (2005)

[Fal85] Falconer, K.J.: The Geometry of Fractal Sets. Cambridge University press, Cambridge(1985).

[Fed96] Federer, H.: Geometric Measure Theory. Springer, Berlin (1996)

[Hahn99] Hahn, U., Micheletti, A., Pohlink, R., Stoyan, D., Wendrock, H.: Stereological Analysis and Modeling of Gradient Structures. J. of Microscopy, **195**,113–124 (1999).

[Hard91] Hardle, W.: Smoothing Techniques. With Implementation in S, Springer-Verlag, New York, (1991).

[JC01] Jain, R. K., Carmeliet, P. F.: Vessels of Death or Life. Scientific American **285**, 38–45 (2001),.

[JM39] Johnson, W.A., Mehl, R.F.: Reaction Kinetics in processes of nucleation and growth. Trans. A.I.M.M.E., **135**, 416–458 (1939).

[K37] Kolmogorov, A.N.: On the statistical theory of the crystallization of metals. Bull. Acad.Sci.USSR, Math.Ser. **1**, 355–359 (1937).

[KF70] Kolmogorov, A. N., Fomin, S. V.:Introductory Real Analysis, Prentice-Hall, Englewood Cliffs (N.J.), (1970).

[Mat75] Matheron, G.: Random Sets and Integral Geometry. John Wiley & Sons, New York, (1975).

[Mol92] Møller, J.: Random Johnson-Mehl tessellations. Adv. Appl. Prob., **24**, 814–844 (1992).

[Mol94] Møller, J.: Lectures on Random Voronoi Tessellations. Lecture Notes in Statistics, Springer-Verlag, New York (1994).

[Pest98] Pestman, W.R.: Mathematical Statistics. An Introduction, Walter de Gruyter, Berlin, (1998).

[Ser03] Serini, G. et al: Modeling the early stages of vascular network assembly. EMBO J., **22**,1771–1779 (2003).

[Silv86] Silverman, B.W.: Density estimation for Statistics and Data Analysis, Chapman & Hall, London, (1986).

[SKM95] Stoyan, D., Kendall, W.S., Mecke, J.: Stochastic Geometry and its Application. John Wiley & Sons, New York, (1995).

[DT17] Thompson, D.W.: On Growth and Form. Cambridge University Press, Cambridge,(1917) .